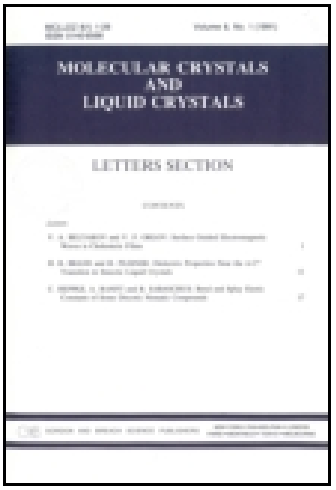

Molecular Crystals and Liquid Crystals
Publication details, including instructions for authors and subscription information:
http://www.tandfonline.com/loi/gmcl20

Electrically Tunable Ophthalmic Lenses for Myopia and Presbyopia Using Liquid Crystals

Hung-Shan Chen[a], Ming-Syuan Chen[a] & Yi-Hsin Lin[a]
[a] Department of Photonics, National Chiao Tung University, Taiwan
Published online: 30 Sep 2014.

To cite this article: Hung-Shan Chen, Ming-Syuan Chen & Yi-Hsin Lin (2014) Electrically Tunable Ophthalmic Lenses for Myopia and Presbyopia Using Liquid Crystals, Molecular Crystals and Liquid Crystals, 596:1, 88-96, DOI: 10.1080/15421406.2014.918321

To link to this article: http://dx.doi.org/10.1080/15421406.2014.918321

Mol. Cryst. Liq. Cryst., Vol. 596: pp. 88–96, 2014

ISSN: 1542-1406 print/1563-5287 online
DOI: 10.1080/15421406.2014.918321

Taylor & Francis
Taylor & Francis Group

Electrically Tunable Ophthalmic Lenses for Myopia and Presbyopia Using Liquid Crystals

HUNG-SHAN CHEN,* MING-SYUAN CHEN, AND YI-HSIN LIN

Department of Photonics, National Chiao Tung University, Taiwan

In this paper, an electrically tunable-focusing and polarizer-free liquid crystal (LC) lens for ophthalmic lenses is demonstrated. The optical operating principles of the LC lens in a human eye system are introduced and the optical principle of the polarization independent of the double-layered LC lens is investigated. The polarization dependency, image quality and the response time of the double-layered LC lens are measured. The continuously tunable-focusing properties of the LC lenses are more practical in applications for different visional conditions of people. The concept in this paper can also be extensively applied to imaging systems, and projection systems, such as cameras in cell phones, pico projectors, and endoscopes.

Keywords Ophthalmic lenses; liquid crystal; vision correction; polarizer-free; myopia; presbyopia

1. Introduction

Liquid crystal lens (LC lens) exhibits electrically-tunable lens power (i.e. an inverse of focal length in an unit of m^{-1}, diopter or D) without any mechanically moving part, light weight, and low power consumption. Many structures and applications of LC lenses are developing, especially for the portable applicat ions of adaptive optics, such as camera systems, pico projection systems, endoscopic systems, zoom systems, and ophthalmic lenses [1–5]. Diffractive Fresnel LC lenses proposed in ophthalmic applications of presbyopia in 2006 [6]. However, such LC lenses require complex Fresnel electrodes (over 200 strips) and have two lens powers only for voltage-off and voltage-on. Moreover, designs for chromatic behavior and aspheric phase profiles are more complicated for diffractive Fresnel LC lenses. As a result, complex Fresnel patterns of diffractive Fresnel LC lenses need to be customized for different people. The performances of human eyes are very different among different people. As a result, it requires developing structure of non-diffractive Fresnel LC lens with large aperture size and polarization independency. In 2013, we demonstrated a polarizer-free LC lens based on double-layered structure whose lens power is continuously tunable and the lens power can be positive and negative [3]. We also introduce the optical principles for applying the tunable focusing LC lenses for presbyopia and myopia to human eye systems. The polarizer-free LC lens we propose can be operated as a positive lens and a negative lens which are also suitable for the application of a tunable eyewear for correcting

*Address correspondence to Hung-Shan Chen, Department of Photonics, National Chiao Tung University, 1001 Ta Hsueh Rd., Hsinchu 30050, Taiwan, R.O.C. E-mail: convince.eo98g@g2.nctu.edu.tw

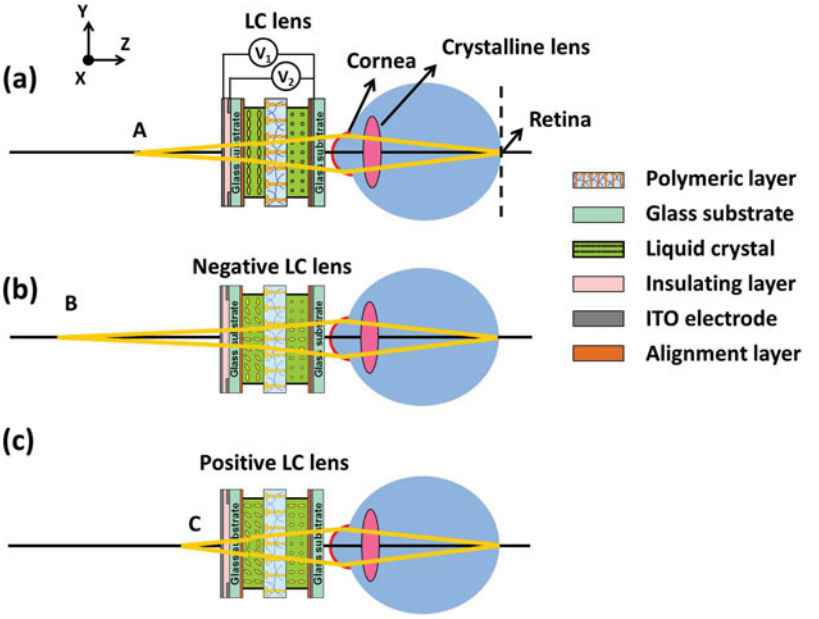

Figure 1. The illustration of operating principles of electrically tunable ophthalmic lens using the polarizer-free LC lens. (a) When the LC lens is at voltage-off state and the crystalline lens is relaxed, the farthest point the eye can see is point A. (b) When the LC lens is operated as a negative lens and the crystalline lens is still relaxed, the farthest point can be furthered extended to point B. (c) When the LC lens is operated as a positive lens and the crystalline lens is still relaxed, the nearest point the eye can see is point C.

myopia and presbyopia. However, the detail measured results of polarization dependency and spatial frequency have not been reported. In this paper, the optical principle of the polarization independent of the double-layered LC lens is investigated. The polarization dependency, image quality and the response time of the double-layered LC lens are measured. The concept in this paper can also be extensively applied to imaging systems, and projection systems, such as cameras in cell phones, pico projectors, and endoscopes.

The human eyes consist of cornea with fixed lens power, crystalline lens with tunable lens power, and retina as an image sensor. The performances of eyes degrade due to refractive anomalies and then result in myopia and hypermetropia. However, presbyopia mainly originates from the age-related degradation of the crystalline lens and then affects the focusing abilities of the eyes, so-called amplitude of accommodation [7]. Such an amplitude of accommodation decreases linearly with the age and then turns out static (around 0 to 2D diopter, or m^{-1}) after age of 50 [8]. Fig. 1(a)–1(c) show the operating principles of electrically tunable ophthalmic lenses for myopia and presbyopia using liquid crystals. The simplified image system of the human eye and LC lens is depicted. In Fig. 1(a), the image system consists of LC lens, cornea, crystalline lens, and a retina as an image sensor. The structure of such a LC lens is also depicted in Fig. 1(a). It consists of Indium Tin Oxide (ITO) electrodes, an insulating layer of polymer NOA81 (Norland), two glass substrates, alignment layers of polyvinyl alcohol (PVA), two LC layers and a polymeric layer to separate two LC layers. The function of the polymeric layer can not only align LC directors, but also be a cell separator; meanwhile, the optical properties of the polymeric

layer are also polarization independent. In addition, the operating scheme of the LC lens is also described in Fig. 1(a)-1(c). In Fig. 1(a), when the applied voltages $V_1 = V_2 = 0$, the LC directors are all aligned parallel to the glass substrates. As a result, the spatial distribution of refractive indices is uniform and the LC lens has no lensing effect. In Fig. 1(b), when $V_2 > V_1$, the LC directors around the rim of the aperture are more parallel to the glass substrates and the LC directors inside the aperture are more perpendicular to the glass substrates. The LC lens is a negative lens because of the gradient refractive index distribution of the LC directors. Similarly, the LC lens is a positive lens when $V_2 < V_1$, as shown in Fig. 1(c). By changing the magnitude of the voltages, the focal length of the LC lens is electrically switchable. The crystalline lens is assumed to be relaxed in Fig. 1(a)–1(c). In Fig. 1(a), when the LC lens is off (the LC lens power is 0D), the farthest point the eye can see is point A when the human eye is nearsighted. When the LC lens is operated as a negative lens, the negative lens power of the LC lens can compensate the positive lens power resulting from myopia. Hence, the farthest point can be extended to point B, as shown in Fig. 1(b). In Fig. 1(c), when the LC lens is operated as a positive lens, the total lens power of the imaging system of human eyes increases. Therefore, the nearest point the eye can see turns out point C which is closer to the eye.

The optical principles of polarization independency of the double layered LC lens are as follows. The electric field of light at normal incidence can be expressed as:

$$E_i = A_x \cdot \hat{x} + A_y \cdot \hat{y}, \tag{1}$$

where A_x and A_y are two complex numbers, and $\hat{x}$ and $\hat{y}$ are unit vectors along the x and y direction in Fig. 1(a). In our previous works, we investigated and demonstrated the polarization independent phase modulation using a double layered structure [9]. Because the applied inhomogeneous electric fields results in the inhomogeneous orientations of LC directors, the outgoing light after the light passes through the double layered LC lens with a given applied voltage can be expressed as Eq.(2):

$$\sum_{r=-R}^{+R} E'_o = \sum_{r=-R}^{+R} e^{i\times\frac{2\pi}{\lambda}\times(n_{eff}(\theta(r),\psi)+n_{eff}(\theta(r),\psi+\frac{\pi}{2}))\times d} \times (A_x \cdot \hat{x} + A_y \cdot \hat{y}), \tag{2}$$

where λ is the wavelength, d is the cell gap, $n_{eff}(\theta(r),\psi)$ is the effective refractive index of the LC as a function of tilt angle of $\theta(r)$ and twist angle (ψ) of the LC directors. R is the radius of the LC lens and r represents position. According to Eq. (2), the polarization of the output light remains the same at a given applied voltage. Furthermore, the spatial phase difference between the center and the border of the aperture of the double layered LC lens can be expressed as:

$$\Gamma_{b,c} = \left[\frac{2\pi}{\lambda} \times ((n_{eff}(\theta(r), \psi) + \left(n_{eff}\left(\theta(r), \psi + \frac{\pi}{2}\right)\right) \times d\right]_b - \left[\frac{2\pi}{\lambda} \times ((n_{eff}(\theta(r), \psi) + \left(n_{eff}\left(\theta(r), \psi + \frac{\pi}{2}\right)\right) \times d\right]_c, \tag{3}$$

In fact, $(n_{eff}(\theta(r), \psi + \frac{\pi}{2})$ equals to n_o. To satisfy the approximation of a thin lens in Geometrical Optics, the distribution of the spatial phase difference in Eq. (3) should be

parabolic. Hence the lens power of the double layered LC lens (P_{LC}) can be expressed as:

$$P_{LC} = \frac{\Gamma_{b,c} \times \lambda}{\pi \times r^2} = \frac{2 \times (n_{eff}(\theta(r_b), \psi) - n_{eff}(\theta(r_c), \psi)) \times d}{r^2}. \quad (4)$$

The tilt angles of LC directors can be adjusted by applied electric fields. As a result, $P_{LC}$is voltage dependent. In Eq. (4), the maximum positive lens power of the double layered LC lens can be achieved by arranging the effective refractive index of LC at the border and the center as n_o and n_e, respectively. As a result, the maximum positive lens power is: $\frac{2 \cdot \Delta n \cdot d}{r^2}$ $\frac{2 \cdot \Delta n \cdot d}{r^2}$, where $\Delta n = n_e - n_o$ is the birefringence of the LC materials. Similarly, the maximum negative lens power is $-\frac{2 \cdot \Delta n \cdot d}{r^2}$. Therefore, the double-layered LC lens is polarization independent, the lens power is electrically tunable, and the maximum lens power depends on the birefringence of LC materials.

2. Experimental Results and Discussions

In order to design polarizer-free LC lenses, a polarization independent LC phase modulation is required. Many polarization independent LC phase modulations are proposed, including residual phase type, double-layered type, mixed type which mix the residual phase type with the double-layered type, and the type using optical isotropic materials (e.g. blue phase LC) [9–14]. Among them, the double-layered type of polarization independent LC phase modulations has large phase shift. As a result, we adopt the double-layered type of polarization independent LC phase modulations to design the LC lens structure. The double-layered structure requires the identical thickness of the two LC layers and the orthogonal orientations of the two LC layers. We adopt the structure of the LC lens by adding a polarization-independent polymeric separator whose optical axis is perpendicular to the glass substrate. To prepare the sample of the polymeric layer, we filled the nematic LC (Merck, MLC-2070, $\Delta n = 0.26$), monomer (Merck, RM257), and photoinitiator (Merck, IRG-184) into the empty twist nematic cell (TN-cell) with cell gap of 50 mm. The ratio of the mixture was 20:79:1 wt% for nematic LC, monomer, and photoinitiator, respectively. The rubbing directions of the alignment layers in the empty TN-cell were orthogonal. The filled cell was applied voltages of 300 V_{rms} at f = 1 kHz at 90°C and was exposed to UV light ($\sim$3 mW/cm^2) for 1 hour. After photo-polymerization, the polymer networks are formed and the solid polymeric layer is obtained. Then we assembled the polymeric layer with other ITO substrates coated with alignment layer and hole-patterned-ITO substrates coated with an insulating layer (Norland, NOA81) to construct the structure of the LC lens depicted in Fig. 1. The thickness of the LC layer is controlled by Mylar films with a thickness of 50 μm. The diameter of hole-patterned electrode was 6 mm and the thickness of the glass substrates were 2.1 mm. The thickness of two LC layers (Merck, MLC-2070) was 50 μm.

Figure 2(a), 2(b), and 2(c) show the polymeric layer was observed under two crossed polarizers with a rotation of the polymeric layer. The polymeric layer is dark when the polymeric layer rotates and this indicates the polymeric layer is polarization independent because the polarization state of the incident polarized light is not modulated by the polymeric layer. We also rotated and observed the double-layered LC lens under crossed polarizers, as shown in Fig. 2(e), 2(f), and 2(g). The double-layered LC lens shows the dark state when the double-layered LC lens is rotated 0 degree and 90 degree with respect to transmissive axis of the polarizer. When the rotation angle is 45 degree, the light leakage is

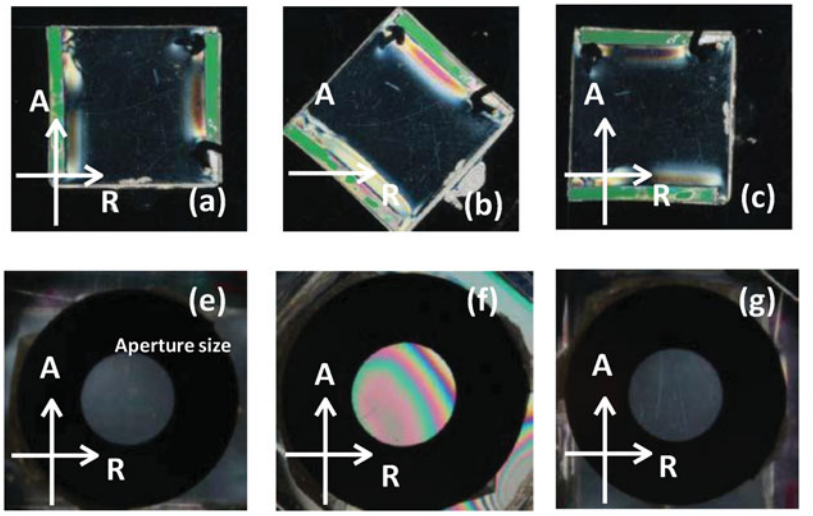

Figure 2. The polymeric layer was observed under crossed polarizers. The polymeric layer rotated (a) 0 degree, (b) 45 degree, and (c) 90 degree. The LC lens was observed under crossed polarizers with a rotation of (e) 0 degree, (f) 45 degree, and (g) 90 degree. The crossed arrows represent the transmissive axes of the polarizer and the analyzer.

observed in Fig. 2(f). This indicates the thicknesses of two LC layers are not identical. From the number of fringes, we estimate the variation of thickness across the aperture. For the green light, it shows around three wavelengths from the center to the edge of the aperture. The variation of the cell gap (or the variation of thickness of the LC layers) is around $3 \times 0.55/0.26 = 6.35$ μm in the LC lens. The variation of cell gap (6.35 μm) is relatively small compared to the thickness of two LC layers of $50 \times 2 = 100$ μm, which is 6.4%. However, the variation of cell gap causes the degradation of the MTF performance.

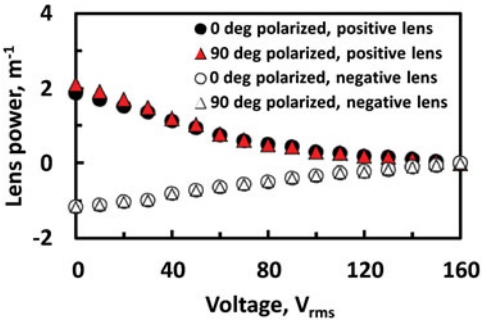

Figure 3. The lens powers of the LC lens as a function of applied voltage under different linearly polarized light. The solid and hollow dots represent the results for 0° linearly polarized light, while the solid and hollow triangles represent the results for 90° linearly polarized light. Black solid dots and red solid triangles represent the positive lens power as a function of V_2 at $V_1 = 160$ V_{rms}. Hollow dots and hollow triangles represents the negative lens power as a function of V_1 at $V_2 = 160$ V_{rms}. $\lambda = 532$ nm.

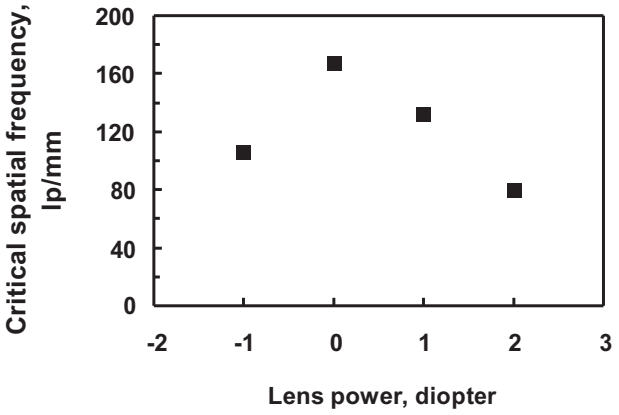

Figure 4. The critical spatial frequency at contrast = 0.5 C_{max} as a function of lens power. The measurement is under ambient white light.

To evaluate the polarization dependency of the double-layered LC lens, the measured lens power of the LC lens as a function of voltage V_1 or V_2 under different linearly polarized light is shown in Fig. 3. The lens power of the LC lens switches from −1.17 D (Diopter or m^{-1}) to +1.88 D for 0^o linearly polarized light, which means the total tunable lens power is 3.05 D for the positive lens. For 90^o linearly polarized light, The lens power of the LC lens switches from −1.17 D (Diopter or m^{-1}) to +2.10 D, which means the total tunable lens power is 3.27 D. According to the results in Fig. 3, the double layered LC lens is nearly polarization independent and the variation of total lens power is less than 7% which may result from the variation of the thicknesses of the two LC layers.

To characterize the imaging performance of the double-layered LC lens, a resolution chart with spatial frequencies ranging from 1 lp/mm to 200 lp/mm was placed 50 cm in front of the double-layered LC lens. The LC lens was attached to the camera (Canon, 500 D with CMOS sensor size: 22.3 mm × 14.9 mm). The modulation transfer function (MTF) was measured at different LC lens powers. To evaluate the imaging qualities of the LC lens, we analysis the contrast (C) of the resolution chart, and the critical spatial frequency as the contrast C is half of maximum contrast is recorded [5]. The higher the critical spatial frequency, the better the spatial resolution of the double-layered LC lens. The experimental results are shown in Fig. 4.The critical spatial frequency of the double-layered LC lens decreases from 167 lp/mm to 106 lp/mm when the lens power is adjusted from 0 D to −1 D. The critical spatial frequency of the double-layered LC lens decreases from 132.5 lp/mm to 79.5 lp/mm with the lens power (1 D to 2 D) when the double-layered LC lens is operated as a positive lens. The results indicate that the resolution or image decreases with the LC lens power. In addition, the image performance of the double-layered LC lens operated as a positive lens (132.5 lp/mm for 1 D) is better than that operated as a negative lens (106 lp/mm for −1 D). The degradation of the MTF results from the aberrations and the variation of the thickness of the two LC layers.

To measure the response time, we measured the response times of the LC lens under different applied voltages. The experimental results are listed in Fig. 5. When the LC lens switches from a negative lens to a positive lens by switching the voltage pairs from (V_1, V_2) = (0 V_{rms}, 160 V_{rms}) to (V_1, V_2) = (160 V_{rms}, 0 V_{rms}), the measured response time is around 0.99 sec. When the LC lens switches from a positive lens with (V_1, V_2) =

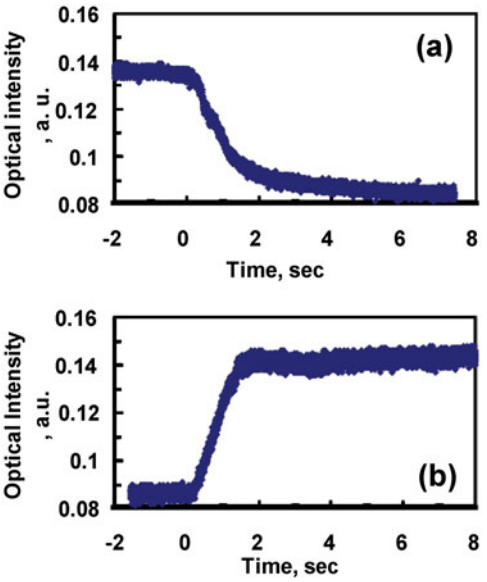

Figure 5. The response times of the double-layered LC lens for switching (a) from a negative lens (−1.2 D) to a positive lens (2 D), and (b) from a positive lens (2 D) to a negative lens (−1.2 D). $\lambda =$ 532 nm.

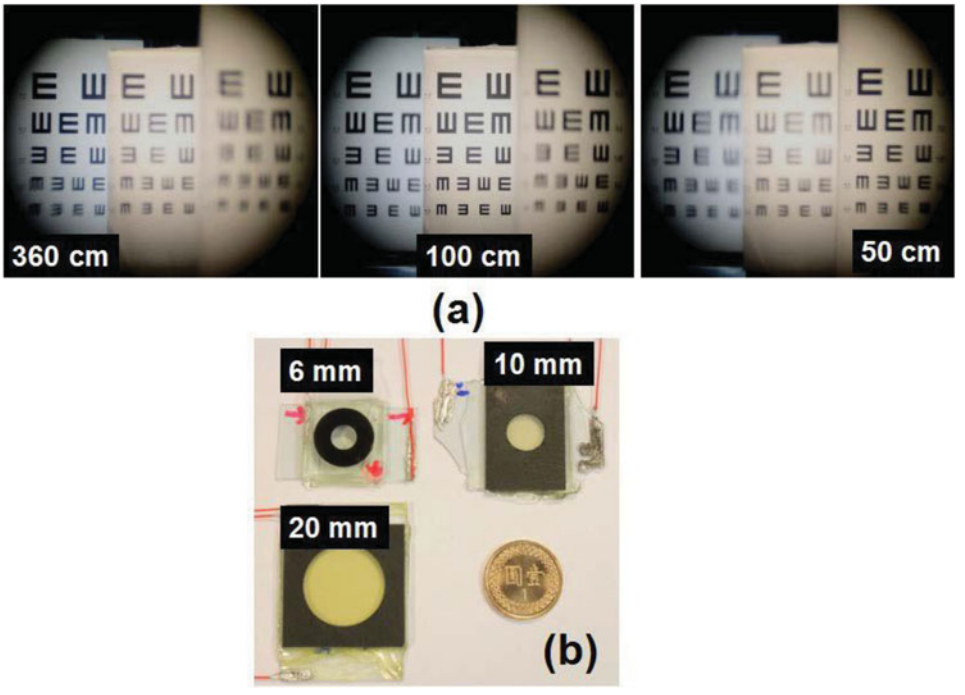

Figure 6. The image performance of the double-layered LC lens. (a)The object at 360 cm is clear when $P_{LC} = -1$ D, the object at100 cm is clear when $P_{LC} = 0$ D, and the object at 50 cm is clear when $P_{LC} = 2$ D. (b) The photo of the developed polarizer-free LC lenses with different aperture size.

(160 V_{rms}, 0 V_{rms}) to a negative lens with (V_1, V_2) = (0 V_{rms}, 160 V_{rms}), the measured response time is 2.69 sec. The response times of the polarizer-free double-layered LC lens is around 3.68 sec which can be improved 4X faster by improving driving methods or by adopting high birefringence LC materials to reduce the cell gaps.

In Fig. 6(a), we also measured the image performance of the double layered LC lens with aperture size of 6 mm for the object charts placing at 50 cm, 100 cm, and 360 cm away from the double layered LC lens. Without the aid of the LC lens power ($P_{LC} = 0$ D), we set the image system to mimic the case of a myopic eye and the farthest point eye can see is at 100 cm (i.e. point A in Fig. 1(a)). With the aid of the negative lens power of -1 D of the double layered LC lens, the farthest point the eye can see is at 360cm which is more extended. The nearest point the eye can see can be closer to 50cm with the aid of a positive lens power of 2 D. Detail discussions of the imaging distance and the measurement can be found in our previous works [5]. In fact, we have also developed the double layered LC lens with different aperture sizes of 6 mm, 10 mm and 20 mm, as show in Fig. 6(b). To enlarge the lens power, multi-layered structure and high refractive index materials are adopted. The tunable ranges of the lens powers of the LC lenses in Fig. 6(b) are: -1 D $\sim +2$ D for the aperture of 6 mm, -2.5 D $\sim +3$ D for the aperture of 10 mm, and -0.4 D $\sim +0.8$ D for the aperture of 20 mm. We are keeping working on polarizer-free LC lens with large aperture size and large tunable range of the lens power for ophthalmic lens applications.

3. Conclusion

An electrically tunable-focusing and polarizer-free liquid crystal (LC) lens for ophthalmic lens is demonstrated. The optical mechanism of a LC lens used in human eye system is introduced and the optical principles of the polarizer-free double-layered LC lens are investigated. To further reduce the voltage, we can use a polymeric layer with a designed spatial distribution of dielectric permittivity [17]. The response time can be improved by driving scheme and improving materials, such as LC and monomer. The concept we proposed can also be applied to other types of lenses, such as liquid lenses based on electro-wetting, as long as the tunable focusing lenses can be operated as a positive and a negative lenses. The concept in this paper can also be extensively applied to other photonic applications, such as cameras in cell phones, pico projectors, and endoscopes.

Acknowledgments

The authors are indebted to Mr. Chia-Ming Chang, Mr. Yu-Jen Wang, and Mr. Michael Chen for technical assistance. This research was supported mainly by Liqxtal Technology Inc. and partially by the National Science Council (NSC) in Taiwan under the contract no. NSC 101-2112-M-009 -011 -MY3.

References

[1] Lin, H. C., & Lin, Y. H. (2010). *Appl. Phys. Lett.*, *97*, 063505.
[2] Lin, H. C., & Lin, Y. H. (2010). *Jpn J Appl Phys*, *49*, 102502.
[3] Lin, Y. H., & Chen, H. S. (2013). *Opt. Express*, *21*, 9428.
[4] Lin, Y. H., Chen, M. S., & Lin, H. C. (2011). *Opt. Express*, *19*, 4714.
[5] Chen, H. S., & Lin, Y. H. (2013). *Opt. Express*, *21*, 18079.
[6] Li, G. Q., Mathine, D, Valley, P., Ayras, P, Haddock, J. N., Giridhar, M. S., Williby, G., Schwiegerling, J., Meredith, G. R., Kipplen, B, Honkanen, S., & Peyghambarian, N. (2006). *Proc. Natl. Acad. Sci.*, *103*, 6100.

[7] Werner, L., Trindade, F., Pereira, F., & Werner, L. (2000). *Arq. Bras. Oftalmol.*, *63*, 503.
[8] Hermans, E., Dubbelman, M., Heijde, R. V. D., & Heethaar, R. (2007). *J. of Vision*, B, 16.
[9] Lin, Y. H., Ren, H., Wu, Y. H., Zhao, Y, Fang, J., Ge, Z, & Wu, S. T. (2005). *Opt Express*, *13*, 8746.
[10] Lin, Y. H., Chen, H. S., Lin, H. C., Tsou, Y. S., Hsu, H. K., & Li, W. Y. (2010). *Appl. Phys. Lett.*, *96*, 113505.
[11] Lin, Y. H., Chen, M. S., Lin, W. C., & Tsou, Y. S. (2012). *J. Appl. Phys.*, *112*, 024505.
[12] Ren, H. W., Lin, Y. H., Wen, C. H., & Wu, S. T. (2005). *Appl. Phys. Lett.*, *87*, 191106.
[13] Lin, Y. H., & Tsou, Y. S. (2011). *J. Appl. Phys.*, *109*, 104503.
[14] Lin, Y. H., Ren, H. W., & Wu, S. T. (2008). *Liq. Cryst. Today*, *17*, 2.
[15] Lin, H. C., Chen, M. S., & Lin, Y. H. (2011). *Trans Electr Electron Mater*, *12*, 234.
[16] Lin, Y. H., Chen, H. S., & Chen, M. S. (2013). *Proc. of SPIE*, *8642*, 86420C.
[17] Lin, H. C., & Lin, Y. H. (2013). *Opt. Express*, *20*, 2045.